



## Effects of cyclic hydraulic pressure on osteocytes

Chao Liu<sup>a</sup>, Yan Zhao<sup>b</sup>, Wing-Yee Cheung<sup>b</sup>, Ronak Gandhi<sup>c</sup>, Liyun Wang<sup>d</sup>, Lidan You<sup>a,b,\*</sup>

<sup>a</sup> Department of Mechanical and Industrial Engineering, University of Toronto, ON, Canada

<sup>b</sup> Institute of Biomaterials & Biomedical Engineering, University of Toronto, ON, Canada

<sup>c</sup> Division of Engineering Science, University of Toronto, ON, Canada

<sup>d</sup> Center for Biomedical Engineering Research, Department of Mechanical Engineering, University of Delaware, Newark, DE 19716, USA

### ARTICLE INFO

#### Article history:

Received 12 November 2009

Revised 2 February 2010

Accepted 3 February 2010

Available online 10 February 2010

Edited by: J. Aubin

#### Keywords:

Osteocyte

Mechanotransduction

Hydraulic pressure

Calcium

Apoptosis

### ABSTRACT

Bone is able to adapt its composition and structure in order to suit its mechanical environment. Osteocytes, bone cells embedded in the calcified matrix, are believed to be the mechanosensors and responsible for orchestrating the bone remodeling process. Recent *in vitro* studies have shown that osteocytes are able to sense and respond to substrate strain and fluid shear. However the capacity of osteocytes to sense cyclic hydraulic pressure (CHP) associated with physiological mechanical loading is not well understood. In this study, we subjected osteocyte-like MLO-Y4 cells to controlled CHP of 68 kPa at 0.5 Hz, and investigated the effects of CHP on intracellular calcium concentration, cytoskeleton organization, mRNA expression of genes related to bone remodeling, and osteocyte apoptosis. We found that osteocytes were able to sense CHP and respond by increased intracellular calcium concentration, altered microtubule organization, a time-dependent increase in COX-2 mRNA level and RANKL/OPG mRNA ratio, and decreased apoptosis. These findings support the hypothesis that loading induced cyclic hydraulic pressure in bone serves as a mechanical stimulus to osteocytes and may play a role in regulating bone remodeling *in vivo*.

© 2010 Elsevier Inc. All rights reserved.

### Introduction

Bone is a living organ that is able to adapt its composition and structure in response to mechanical stimuli [1,2]. It was believed that mechanical forces stimulate bone cells to maintain tissue homeostasis in bone. Mechanical loading induces a variety of physical signals that may stimulate cells, including tissue strain, fluid shear, and fluid pore pressure. Both strain and fluid shear have been extensively studied and shown to significantly affect bone cells *in vitro* [3–8]. There are a few studies that have investigated the effects of fluid pressure *in vivo* and *in vitro* [9–13], suggesting that fluid pressure is a potent stimulus to the bone. Macroscopically, venous stasis or applied pressurization by external loading was associated with increased bone formation [14,15]. At the tissue level, fluid pressure causes increased calcification [16], and inhibition of resorption [17]. Therefore it has been suggested that bone remodeling depends on changes in interstitial fluid pressure [12,18–21]. However, the cellular mechanism of bone's response to fluid pressure is poorly understood.

In this study, we investigated the osteocyte response to pressure using an *in vitro* approach. It has been proposed that osteocytes are the cells that detect mechanical loading in bone [22]. Osteocytes account for 90–95% of bone cells. They are embedded in the mineralized bone matrix, forming an interconnected network [23]. Due to their unique

location and abundance, osteocytes are believed to be responsible for sensing mechanical loading and orchestrating the bone remodeling process.

The fluid pressure experienced by osteocytes *in vivo* is cyclic in nature, the magnitude of which was calculated to be up to 0.27 MPa [24]. Recent studies found that the hydraulic permeability of the bone tissue was smaller than the previous model assumed, leading to an even higher estimation of the hydraulic pressure buildup (~5 MPa) around osteocytes [25–27]. In this study, we subjected MLO-Y4 cells, a well-established osteocyte-like cell line, to a cyclic hydraulic pressure (CHP) with a peak value of 68 kPa and 2 s per cycle. This loading regimen was chosen to be consistent with previous studies [21] and also due to the limit of our loading system (leakage would occur under higher pressures).

Selective responses of osteocytes to CHP were studied, including intracellular  $\text{Ca}^{2+}$  concentration ( $[\text{Ca}^{2+}]_i$ ), cytoskeleton organization, mRNA expressions of cyclooxygenase-2 (COX-2), receptor activator of nuclear factor kappa B (NF- $\kappa$ B) ligand (RANKL), and osteoprotegerin (OPG), and apoptosis. Previous studies have found that other types of mechanical stimuli such as fluid shear stress have altered these outcome measures in bone cells. Intracellular calcium is an early second messenger that plays key roles in a number of metabolic pathways [28]. Changes in  $[\text{Ca}^{2+}]_i$  usually increases within seconds of mechanical stimulation on bone cells [29]. In osteocytes, cell body deformation through mechanical loading induced calcium response [30]. In this study,  $[\text{Ca}^{2+}]_i$  was measured and used as an indicator of responsiveness when osteocytes were subjected to CHP.

\* Corresponding author. 5 King's College Road, Room 314D, Toronto, Ontario, Canada M5S 3G8. Fax: +1 416 978 7753.

E-mail address: [youlidan@mie.utoronto.ca](mailto:youlidan@mie.utoronto.ca) (L. You).

Another early-intermediate event in cellular response to mechanical loading is the changes in cytoskeleton organization. Following mechanical stimulations, cells typically show changes in cytoskeleton organization in 15 min [31]; both actin filament [31], and microtubule [32] have been shown to be integral in mechanotransduction.

Downstream gene and protein expressions are altered hours after mechanical stimulations [21]. Fluid flow applied to MLO-Y4 cells upregulated COX-2, the gene that encodes cyclooxygenase-2, a key enzyme in the production of Prostaglandin E<sub>2</sub> (PGE<sub>2</sub>) [8]. Substrate stretching also upregulated COX-2 [33]. The signaling molecule PGE<sub>2</sub> is implicated in both modeling and remodeling of bone [34]. In addition, two key molecules have been found to mediate osteoclast activity during bone resorption: RANKL and OPG. The rate of bone resorption is dependent on the RANKL/OPG ratio [35].

Furthermore, osteocyte apoptosis is a vital regulator of bone remodeling and a critical determinant of bone strength. Osteocyte apoptosis has been suggested to signal osteoclast recruitment [36,37]. Lack of mechanical loading has been shown to be the major factor that causes osteocyte apoptosis *in vivo* [38]. However the influence of fluid pressure on osteocyte apoptosis has not been well studied *in vitro*.

The aim of this study was to investigate the effects of CHP on osteocytes. We hypothesized that CHP is an important stimulus to osteocytes and would induce significant changes in calcium mobilization, cytoskeleton morphology, gene expression levels for COX-2, RANKL, and OPG, and osteocyte apoptosis. The results from this study bridged a gap in the knowledge of bone remodeling due to mechanical loading. From this knowledge, new pharmaceutical agents and exercise regimens could be developed for more effective treatments of bone diseases such as osteoporosis, enhancing general bone health.

## Materials and methods

### Cell culture

MLO-Y4 osteocyte-like cells (gift from Dr. Lynda Bonewald, University of Missouri-Kansas City, Kansas City, MO, USA) were cultured in  $\alpha$ -Modified Eagle's Medium ( $\alpha$ -MEM, GIBCO™) supplemented with 2.5% fetal bovine serum (FBS, Hyclone), 2.5% calf serum (CS, Hyclone), and 1% penicillin and streptomycin (P/S, GIBCO™) on 100 mm petri dishes coated with type I rat tail collagen (BD Laboratory). The cells were maintained at 37 °C and 5% CO<sub>2</sub> in a humidified incubator (Thermo Scientific). Cell subculture was performed when the cells reached 70% confluence. With the exception of calcium experiments, cells were seeded on type I rat tail coated glass slides (75 mm × 38 mm × 1 mm) 48 h prior to CHP loading at 150,000 cells per slide to ensure 70–80% confluence at the time of experiment. For the apoptosis experiment, the cells were serum starved 24 h prior to CHP loading with  $\alpha$ -MEM containing 0.02% FBS, 0.02% CS, and 1% P/S. For calcium experiment, MLO-Y4 cells were seeded onto non-coated glass slides (75 mm × 38 mm × 1 mm) using the same culturing protocols.

### Cyclic hydraulic pressure loading *in vitro*

MLO-Y4 cells were seeded onto collagen-coated glass slides, which were placed in the pressure chambers and pressure gauges (Omega Inc.) were attached to monitor the pressure inside of the chamber, as described previously [21]. Fresh culture media was used in the experiments for cytoskeleton staining, PGE<sub>2</sub> assay, and quantitative RT-PCR assays. A syringe (KD Scientific), driven by a syringe pump (Cole-Parmer), applies the hydraulic pressure loading directly to the medium filled in the pressure chamber. The cells were subjected to cyclic hydraulic pressure with 0.5 Hz triangular waveform which has peak pressure of 68 kPa for 1 or 2 h. The loading regime used in this study was within the range of pressures used in other studies [15,21,24,39–43]. Due to the relative incompressibility of the aqueous medium, a very small volume change (<0.5 mL) was used to induce the

desired pressure. This small volume was found to result in a negligible shear stress. The peak shear stress was estimated to be  $4.9 \times 10^{-3}$  Pa, using equation  $\tau = 6\mu Q / (bh^2)$ , where  $\tau$  is the shear stress;  $\mu$  is the viscosity of the medium, which is approximated to be that of the water at room temperature ( $1 \times 10^{-3}$  Pa s);  $Q$  is the flow rate, which is 0.5 ml/s as a result of the syringe displacement;  $b$  is the flow channel width, which is 38 mm;  $h$  is the flow channel height, which is 4 mm. The calculated maximum shear stress level experienced by the cells was at least 2 orders of magnitude lower than those that are known to excite bone cells *in vitro* [44]. Therefore, the responses observed in the present study were attributed to the hydraulic pressure.

As control, collagen-coated glass slides seeded with MLO-Y4 cells were placed in pressure chambers but without application of CHP. The pressure experiments were performed at room temperature.

### Real-time intracellular calcium measurement

Intracellular calcium ion concentration was quantified as previously described [45]. Briefly, prior to exposure to CHP, MLO-Y4 cells on quartz slides were incubated with 10  $\mu$ M Fura-2AM (Molecular Probes, Eugene OR) for 30 min at 31 °C (to reduce dye compartmentalization), then washed with fresh working medium ( $\alpha$ -MEM without phenol-red (GIBCO™) supplemented with 1% FBS and 1% CS). The slides were placed into a custom-made pressure chamber (Fig. 1), and fixed to a pre-heated stage (31 °C) on an inverted microscope (Eclipse Ti-S, Nikon, Japan) with a calcium imaging system (PTI EasyRatioPro system, USA). For 30 min, the cells were left undisturbed. Fresh working medium was used during the pressure experiment. During the application of pressure loading, Fura-2 340 nm/380 nm ratio values were converted to  $[Ca^{2+}]_i$  values using image analysis software (EasyRatio, PTI). Baseline  $[Ca^{2+}]_i$  level was recorded for 3 min, followed by application of CHP for 3 min. Images were recorded at a rate of one every 160 ms ( $n = 30$ ). Temporal profiles were determined for approximately 30 cells per field of view. Each cell was classified as responding or not responding: a responding cell was defined as having transient increases in the  $[Ca^{2+}]_i$  of at least two-fold increase in the Fura-2 340 nm/380 nm ratio over the maximum oscillation recorded during the 3 min baseline period.

### Cytoskeleton immunostaining and quantification

MLO-Y4 cells were exposed to CHP loading or non-loading (static control) for 1 h, and then their actin filament and microtubules staining were performed as previously described [21] ( $n = 8$ ). To stain the actin filaments, the cells were fixed with 3.7% Formaldehyde in PBS for 10 min, then permeabilized with 0.1% Triton X-100 in PBS for 5 min. The cells were stained with Alexa Fluor 488 phalloidin (Molecular Probes A-12379). To stain the microtubules, the cells were fixed with 0.25% glutaraldehyde and permeabilized with 0.1% Triton X-100 in PHEM buffer (25 mM HEPES, 60 mM PIPES, 10 mM EGTA, 2 mM MgCl, pH 6.9, warmed to 37 °C) for 30 min. Following fixation, cells were quenched in 2  $\mu$ g/ml of sodium borohydride for 15 min. The fixed cells were treated with 10% BSA for 1 h to reduce non-specific binding. Microtubules were first labeled with alpha-tubulin antibody (AB Cam, Cambridge, MA, USA) for 3 h, and then with FITC secondary antibody (Invitrogen) for 1 h. Cells were then imaged using a laser scanning confocal microscope (Olympus, USA). The buckling points in microtubules were quantified using a chord-to-point distance accumulation (CPDA) method [46]. A square ROI of 150 × 150 pixels was selected on the microtubule immunofluorescent images of the cell, which covers around 30% of the cell area. The buckling regions in the ROI were counted and the curvature at each buckling region was calculated.

### mRNA quantification

Immediately after CHP loading, both of the loaded and control MLO-Y4 cells on glass slides were trypsinized. The total RNA was

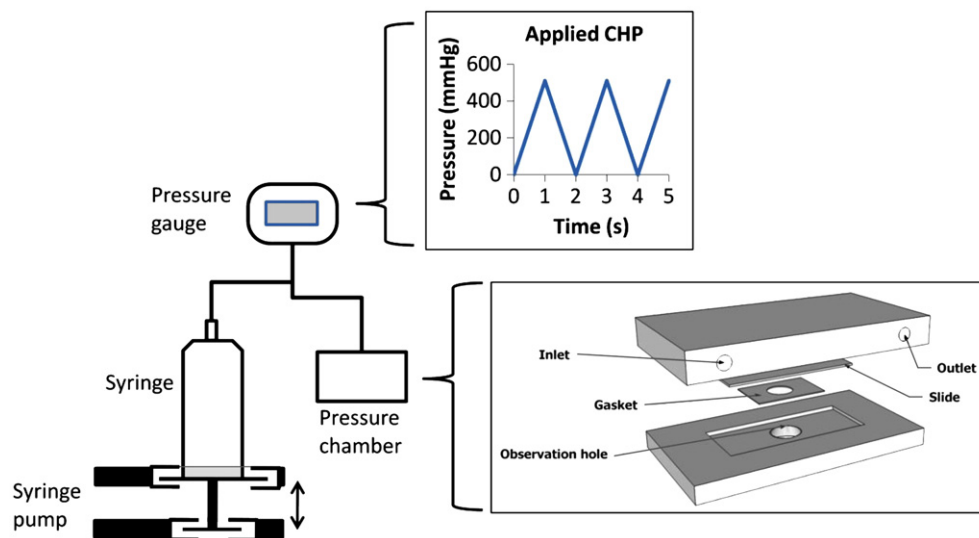


**Fig. 1.** A syringe driven by a programmable pressure pump was used to apply CHP (0 to 68 kPa, at 0.5 Hz) to cells. The pressure inside the chamber was continuously monitored through a pressure gauge to ensure that the desired loading profile was applied. A slightly modified pressure chamber was used for real-time intracellular  $[Ca^{2+}]_i$  observation. The top and bottom halves of the chamber were secured with screws. The gasket, sealed with vacuum grease, prevents leakage of media inside the chamber. The microscope objectives were able to focus on the glass slide through the observation hole.

extracted from cells ( $n = 12$ ) using RNeasy Mini Kit (Qiagen, USA). The extracted RNA was treated with DNase I (Fermentas) and reverse-transcribed using SuperScript<sup>TM</sup> III RT (Invitrogen, USA) to synthesize cDNA. For genes COX-2, RANKL, OPG, and 18 S, Quantitative PCR (qPCR) was used to amplify the cDNA of the samples using gene-specific primers and SYBR Green I (Roche, USA) in Mastercycler ep Realplex<sup>2</sup> (Eppendorf, USA). The copy number of COX-2, RANKL, and OPG for each experimental group were normalized to its 18 S (housekeeping gene) rRNA levels and the control group. To define the time courses of the gene expressions, the duration of the CHP stimulation was varied at 1 or 2 h.

#### Apoptosis staining and quantification

To assess the effects of CHP on osteocyte apoptosis, apoptosis in MLO-Y4 cells was induced by serum starvation of the cells with  $\alpha$ -MEM containing 0.02% FBS, 0.02% CS and 1% P/S for 24 h prior to the application of CHP. CHP was applied for 1 h to these serum starved MLO-Y4 cells, during which cells were exposed to fresh complete medium. Then they were incubated for 1 h at 37 °C and 5% CO<sub>2</sub> with fresh complete medium. The percentage of apoptotic cells was measured at prior to CHP loading (24 h after the start of serum starvation), and compared against cells that were exposed to complete media. Apoptosis was measured again immediately after CHP (25 h post the beginning of serum starvation) or with 1 more hour of incubation in fresh complete medium (26 h post the beginning of serum starvation) and compared with non-loaded controls (cells in pressure chambers without pressure loading application) ( $n = 8$ ). The APOPercentage dye (Biocolor Ltd.) was used to stain the apoptotic cells. The APOPercentage dye can only be actively transported into the cells that lose their membrane asymmetry, which occurs early during apoptosis [47]. The accumulation of APOPercentage dye stains the apoptotic cells pink, allowing detection of apoptosis using a microscope. PAP pen (Sigma) was used to draw a containment oval on slides of cells subjected to either CHP or static controls. The hydrophobic ovals served as a barrier to control the staining area during the 30 min staining process. The dye stock solution was diluted (1:20) in complete medium, and the diluted dye (50  $\mu$ L) was applied inside the oval barrier region. After the 30 min incubation, the dye was removed. The region was then rinsed twice with 1 mL of PBS. The cells were immersed in PBS before being

photographed under a microscope. Five regions within the oval region were photographed. The cells in these photos were quantified for the number of apoptotic cells over the total number of cells in each field of view (FOV). All cells were counted using the ImageJ software with the cell counter plug-in.

#### Statistical analysis

Student *t*-tests (performed with SPSS software) were used to determine significant differences between CHP loaded groups and static groups (control). Statistical significance was defined as  $P < 0.05$  (two tailed).

## Results

#### Increased oscillations of intracellular calcium concentration

The increase in  $[Ca^{2+}]_i$  during application of CHP loading was observed 40 s after the start of the loading (Fig. 2A). Few cells showed increases in  $[Ca^{2+}]_i$  during the baseline period. Upon the application of CHP, a significantly ( $P = 0.002$ ) higher percentage of cells (20.9%) showed over two-fold increase in  $[Ca^{2+}]_i$  (Fig. 2B). Oscillations in  $[Ca^{2+}]_i$  were observed in all cells even after the CHP loading was stopped.

#### Altered microtubule morphology but with no changes in actin filament

Fluorescent staining using Alexa Fluor 488 phalloidin for actin filament showed no significant difference between MLO-Y4 cells that were subjected to CHP versus non-loaded controls (Fig. 3A). No obvious stress fiber formation was observed. However, after applying CHP to MLO-Y4 cells, the microtubules showed increased buckled structure (Fig. 3A). The number of buckling regions and the curvatures of these regions were computed using the CPDA algorithm implemented in MatLab. There was a 4.4-fold increase in the curvatures of microtubule buckling points ( $P = 0.049$ ) (Fig. 3D). However the number of detected corners, which corresponds to the number of buckling points in the microtubules, remained the same for both groups (Fig. 3C).

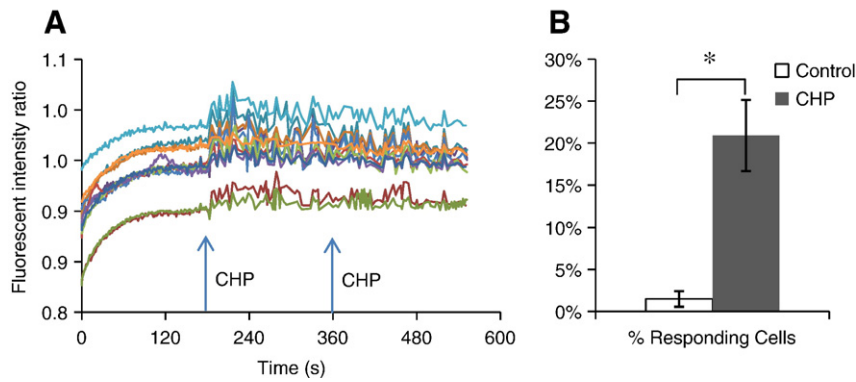


**Fig. 2.** (A) The observed 340/380 nm fluorescent intensity ratio in representative cells. Before the application of pressure, 180 s of baseline was recorded. CHP was applied at the 180 s mark. Fluorescent intensity ratio level, which corresponds to intracellular  $[Ca^{2+}]$ , showed first peak at 36 s after the start of CHP application. (B) Effect of CHP on intracellular  $[Ca^{2+}]$  in MLO-Y4 cells ( $n = 30$ ). Significantly ( $P = 0.002$ ) more cells showed more than two-fold increase in intracellular  $[Ca^{2+}]$  when treated with CHP compared with non-loaded cell (control).

*Increased COX-2 expression*

We measured the relative mRNA expression level of COX-2, which is vital for the synthesis of PGE<sub>2</sub> in the cell [48–50]. Following the

loading regime of 68 kPa at 0.5 Hz for 1 h, COX-2 mRNA expression level increased by 65% in CHP loaded cells ( $P = 0.006$ ), compared with non-loaded controls (Fig. 4A). However the elevated COX-2 level was abolished after 2 h of CHP (68 kPa, 0.5 Hz) loading. There was no

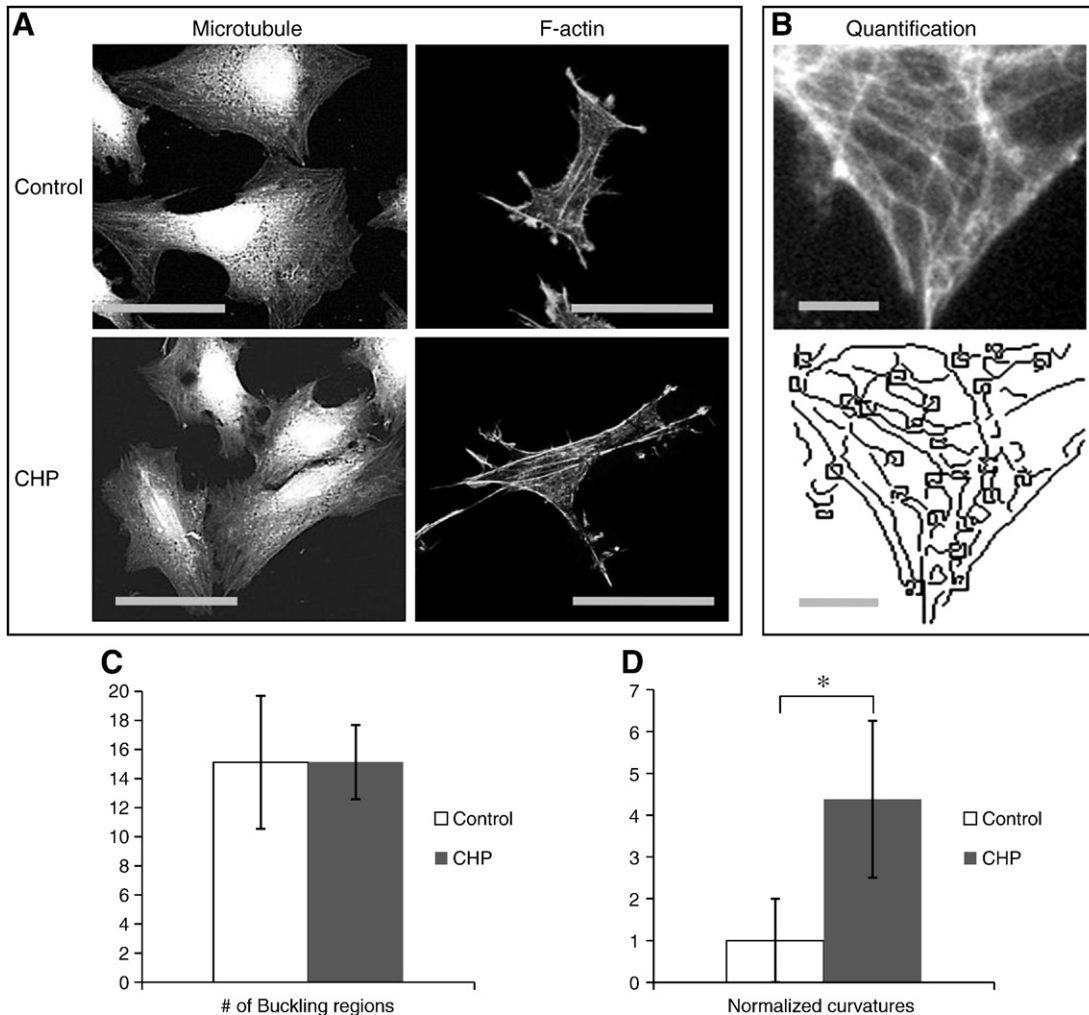


**Fig. 3.** (A) Effect of CHP (68 kPa at 0.5 Hz for 1 h,  $n = 8$ ) on the actin filament and microtubule morphology in MLO-Y4 cells (bar = 30  $\mu$ m). The microtubules showed more bended structures after the application of CHP, while the actin filament organization remained the same between the control and CHP treated groups. (B) An example of the CPDA analysis is shown (bar = 10  $\mu$ m). The ROI (top panel) consists of an area of 150  $\times$  150 pixel (38.8  $\times$  38.8  $\mu$ m). A MatLab program implementing the CPDA algorithm was used to find the buckling regions and the curvature of each buckling region (bottom panel of B). (C, D) Quantification of microtubule buckling regions after 1 h CHP loading on MLO-Y4 cells ( $n = 8$ ). (C) No significant difference was observed in the number of microtubule buckling regions. (D) The curvature in each of the buckling regions was calculated and normalized to the no pressure condition (control). The cells treated with CHP showed significantly larger curvature compared with non-treated cells (control) ( $P = 0.049$ ).

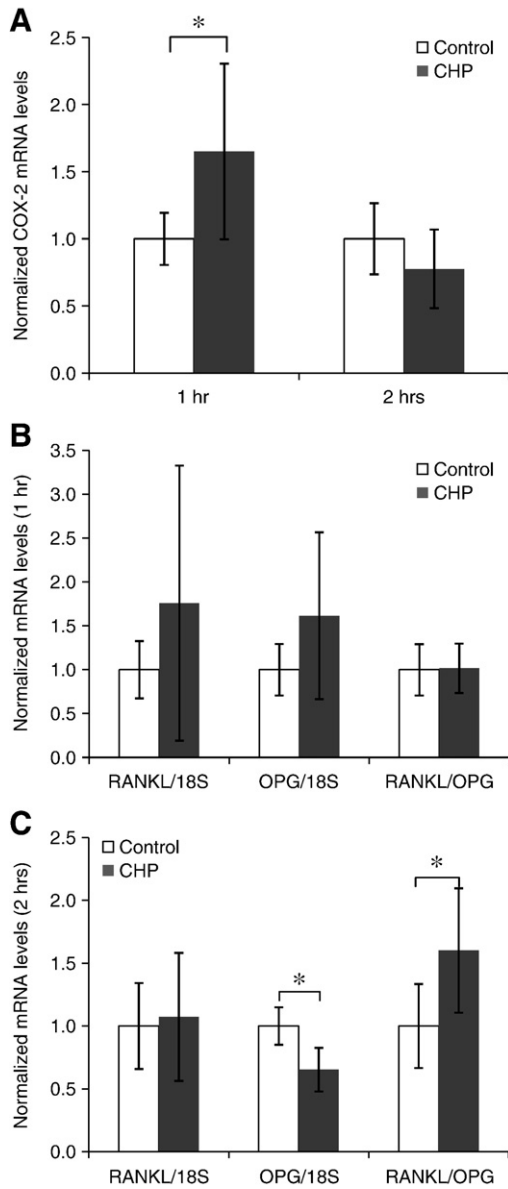


**Fig. 4.** (A) Relative mRNA levels of COX-2 ( $n = 12$ ). After 1 h of CHP (68 kPa, 0.5 Hz) the relative expression of COX-2 mRNA in cells subjected to CHP was 1.75 times higher than that in non-loaded controls ( $P = 0.006$ ). However this difference disappeared after 2 h of CHP. (B, C) Relative mRNA levels of OPG, RANKL and RANKL/OPG in MLO-Y4 cells ( $n = 12$ ) after 1 h (B) and 2 h (C) of CHP loading (68 kPa, 0.5 Hz). Sham loaded glass slides seed with MLO-Y4 cells were used as no pressure control. No significant difference was observed in OPG, RANKL expression level, or RANKL/OPG ratios after 1 h of CHP (B). However the OPG expression level decreased by 35% ( $P = 0.001$ ), and caused the RANKL/OPG ratio in CHP treated cells increased by 82% after 2 h compared to the controls ( $P = 0.02$ ).

significant difference in COX-2 gene expression between the CHP and control groups after 2 h of loading.

#### RANKL/OPG expression

Opposite to the case of COX-2, the mRNA expression levels of OPG and RANKL did not show any significant change in MLO-Y4 cells and the RANKL/OPG ratio showed a slight but not statistically significant decrease after 1 h of CHP loading (68 kPa, 0.5 Hz) (Fig. 4B). Increasing the duration of the CHP loading to 2 h, the expression levels of RANKL still did not show any significant difference from the controls. However, the prolonged stimulation did result in a significant decrease (35%,

$P = 0.001$ ) in the OPG mRNA level, and a significant increase in the RANKL/OPG ratio (60%,  $P = 0.02$ ) (Fig. 4C).

#### Decreased osteocyte apoptosis

After 24 h of serum starvation, the percentage of apoptotic cells was 26.5%, compared with 11.8% of cells cultured with complete medium for the same duration ( $P = 0.047$ ) (Fig. 5A). To determine whether CHP can inhibit the osteocyte apoptosis induced by serum starvation, we applied 1 h CHP on MLO-Y4 cells after 24 h serum starvation. The control group was serum starved for 24 h and then placed in the pressure chamber for 1 h without pressure loading. At the beginning of this 1 h post serum starvation, fresh complete medium was provided to both CHP and control groups. We found that immediately after applying CHP for 1 h (25 h from the start of serum starvation), the percentages of apoptotic cells were not significantly different from those of non-loaded groups (Fig. 5B). However, after an additional 1 h incubation (26 h from the start of serum starvation), there was a 50% decrease in the percentage of apoptotic cells ( $P = 0.006$ ) in the CHP loaded (4.7%) compared with the control (9.3%) groups (Fig. 5B). The percentage of apoptotic cells in the control groups did not change significantly after 1 h of incubation. However, 1 h incubation following the CHP treatments resulted in a significant (19%) reduction in apoptotic cells ( $P = 0.01$ ) compare with CHP treatment alone. Both CHP loaded and control groups show

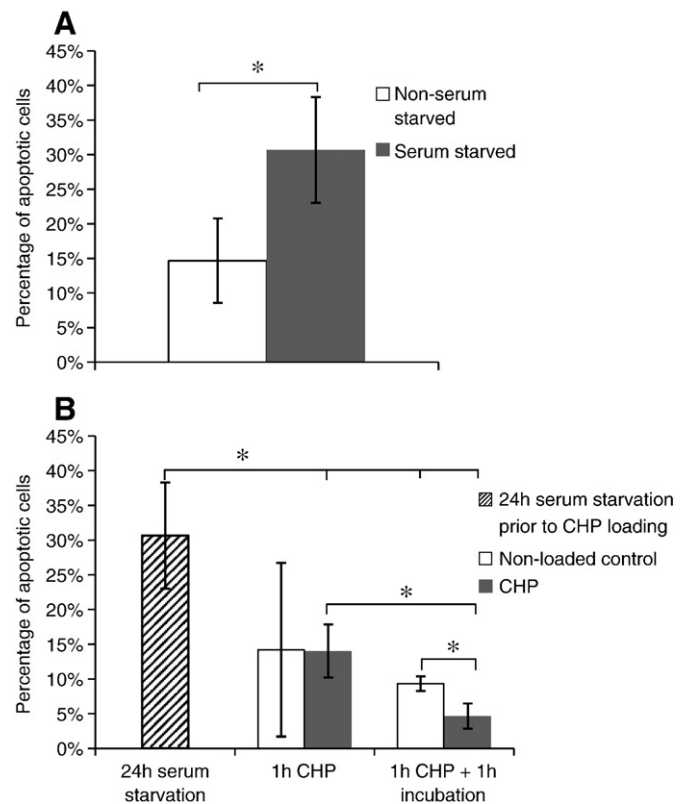


**Fig. 5.** (A) The percentage of apoptotic MLO-Y4 cells after 24 h of serum starvation, compared with cells under normal conditions ( $n = 6$ ,  $P = 0.08$ ). (B) The percentage of apoptotic MLO-Y4 cells after 1 h of CHP ( $n = 8$ ) and with 1 additional hour of incubation. In both CHP and control groups, the percentage of apoptotic cells significantly decreased after 1 h CHP + 1 h of incubation compared with the percentage of apoptotic cells after 24 h of serum starvation ( $P = 0.0022$  for Control,  $P = 0.0010$  for CHP). The percentage of apoptotic cells between CHP and control was not significantly different immediately after 1 h of CHP. But after an additional 1 h incubation, the CHP treated groups (4.7%) had significantly ( $P = 0.006$ ) less percentage of apoptotic cells compared to control groups (9.3%). Also, compared with cells at 25 h, the cells subjected to CHP had lower percentage of apoptotic cells with 1 more hour of incubation ( $P = 0.011$ ).

significant decreases in percent of apoptotic cells at 26 h after the start of serum starvation (Fig. 5).

## Discussions

Mechanical loading produces multiple physical signals that may stimulate bone cells and eventually lead to bone adaptation and remodeling. Cellular responses to some of the stimuli such as fluid shear stress and substrate stretching are relatively well studied. One of the knowledge gaps is whether and how osteocytes sense cyclic hydraulic pressure. In this study, we investigated the responses of osteocytes to cyclic hydraulic pressure (CHP) associated with *in vivo* functional loading. In specific, we showed an increase in  $[Ca^{2+}]_i$  of MLO-Y4 osteocyte-like cells in response to CHP. The buckling in the osteocyte microtubules showed increased curvature after CHP loading. At the mRNA level, COX-2 expression increased after 1 h of CHP loading; RANKL/OPG ratio showed significant increase after 2 h of CHP loading. Lastly, we observed a beneficial effect of CHP that reduced osteocyte apoptosis induced by serum starvation.

The increase in  $[Ca^{2+}]_i$  was observed under CHP stimulation but the increase was not as rapid compared to when osteocytes were subjected to fluid flow (Fig. 2A). The  $[Ca^{2+}]_i$  level increased after about 40 s from the start of the loading. In contrast, bone cells responded much faster under fluid shear stress stimulation, with increased  $[Ca^{2+}]_i$  after about 20 s of loading [51]. This observation suggests that osteocytes may have a different mechanism of sensing hydraulic pressure. Compared with the mostly single peak response of fluid shear treated cells [51], CHP treated MLO-Y4 cells from the present study had a longer, oscillatory response. It is not clear what is the upstream event triggering this elevated  $[Ca^{2+}]_i$  response. It has been shown that transient receptor potential (TRP) channels can be activated by hypo-osmotic stimulation and induce calcium ion influx in osteoblasts [52]. It is possible that similar mechanism exists in osteocyte as well, which is responsible for the observed increase in  $[Ca^{2+}]_i$  in our study. Being an early secondary messenger, increase in  $[Ca^{2+}]_i$  could set off an array of downstream biochemical responses in bone cells, including autocrine and paracrine signaling [45,53]. The increase in  $[Ca^{2+}]_i$  has been found to cause translocation of nuclear factor  $\kappa$ B to the nucleus and stimulate COX-2 expression in osteoblasts [54]. Therefore it is possible that  $[Ca^{2+}]_i$  could be the cause of the elevated COX-2 mRNA expression observed in this study. It is also identified that increase in  $[Ca^{2+}]_i$  could activate ERK and p38 MAPK in osteoblast [53]. It might be possible that ERK and p38 MAPK is activated by elevated  $[Ca^{2+}]_i$ , and this may have caused the observed increase in COX-2 expression in our study as well. There is also evidence that  $[Ca^{2+}]_i$  could modulate microtubule morphology [55]. It is possible that the loading induced  $[Ca^{2+}]_i$  release and changes in microtubule morphology could form a positive feedback loop that reinforces the responses of osteocytes to CHP.

The actin filament organization did not change after application of CHP, in contrast to the stress fiber formation after fluid flow [8]. However, we demonstrated that cyclic pressure loading at 68 kPa at 0.5 Hz was able to cause changes in the microtubule organization in MLO-Y4 osteocyte-like cells. In cells without external loading, microtubules have been shown to be in the state of constrained buckling with multiple buckling regions with straight segments in between [56]. From the present study, the curvatures of the bending sections in the microtubules showed significant increase in cells subjected to CHP, indicating that the buckling sections of the microtubules became more 'compressed' after CHP loading. Interestingly, the number of detected corners, which corresponds to buckling sections, did not increase. Several factors could contribute to this observed change in the microtubule morphology as follows: 1) Since very high pressure (100 MPa) was needed to denature proteins [57], it is more likely that the change in microtubule is a regulatory response of the cells. Calcium, which showed increased intracellular concen-

tration in our study, has been shown to promote microtubule depolymerization [58]. 2) The change in microtubule morphology could be also related to the PGE<sub>2</sub> level. It has been shown that microtubule is an integral part for PGE<sub>2</sub> release in osteocytes [59]. 3) Changes in cytoplasmic streaming may also change the dynamics of the microtubule network, since it was shown to be affected by fluid pressure [60]. 4) The cell membrane is an often overlooked cell structure that may sense pressure loading in cells. Pressure could change the spacing between the lipid bi-layers and its fluidity, which would affect membrane-bound receptors. Further studies are warranted to elucidate the molecular mechanisms of the osteocyte responses to CHP.

We showed that COX-2 expression increased after applying CHP loading to MLO-Y4 cells for 1 h (Fig. 4A). It is in agreement with a previous study in which the effects of CHP on osteoblast-like (MC3T3-E1) cells were studied [21]. The increase in COX-2 may suggest increased level of PGE<sub>2</sub> and its release into extracellular space, which may produce autocrine effects to i) enhance osteocyte response to mechanical loading [61], and ii) enhance osteoblast differentiation [62], leading to increased bone formation [63–65]. It has also been shown to mediate resorption [66]. In our study, the increase in COX-2 disappeared after 2 h of CHP. This result is actually in agreement with the response induced by substrate stretching, which showed a biphasic temporal profile of COX-2 response [33]. Our study showed that COX-2 may be a part of a pathway that can be activated by all three types of mechanical loading (fluid shear stress, substrate stretching and fluid pressure), which may include adenylate cyclases, GTPase, ERK and PKA activation [67].

Both primary osteocytes and MLO-Y4 osteocyte-like cells have been shown to express RANKL and OPG, and were able to modulate osteoclast formation and activation [68]. RANKL and OPG have also been observed to be co-localized with osteocytes *in vivo* [69]. The present study showed that RANKL/OPG ratio did not change after 1 h of CHP loading, but it increased significantly after 2 h of CHP loading. The increase in the RANKL/OPG ratio mainly results from the decrease in OPG expression (Fig. 4C). The canonical Wnt signaling, which regulates OPG expression in osteoblasts [70], might be activated by CHP. Since evidence has shown that osteocyte alone can trigger osteoclast formation [68], the results from this study indicated that long-term CHP of 68kPa level might trigger bone resorption. In contrast, fluid shear stress was shown to induce increases in both RANKL and OPG mRNA and protein expression, and caused the RANKL/OPG ratio to decrease [4,71]. Our results suggest that CHP may modulate osteoclast functions in a manner different from fluid shear.

Similar to the effect of fluid shear stress [72] and substrate stretching [73] on osteocytes, CHP have reduced apoptosis [43]. We have shown here that 1 h of CHP loading was sufficient to produce anti-apoptotic effects, although the reduction in apoptotic cells was detected after 1 h of incubation post application of CHP (Fig. 5B). In our study, exposure to fresh complete medium significantly reduced the percent of apoptotic cells in both CHP and control groups, but CHP loading had a significant more reduction than the non-loaded control. Since the disruption of the asymmetric composition of cell membrane detected by the Apoptosome assay is an early event in the apoptosis process [47], it was likely that a portion of the apoptotic cells was later rescued from apoptosis by CHP. The elevated COX-2 level induced by CHP may have been beneficial for osteocyte viability [61] through Wnt/ $\beta$ -catenin signaling pathway [74]. Our result is consistent with previous studies with bone explants, which showed cyclic hydraulic pressure reduced osteocyte apoptosis [43].

In summary, the present study found that osteocytes were able to detect and respond to cyclic hydraulic pressure *in vitro*. As tested in the present study with a cyclic pressure at 68 kPa level, 20.9% of the MLO-Y4 cells responded to the simulation by increasing the  $[Ca^{2+}]_i$  40 s after the onset of loading. The curvature of the buckling points in microtubules increased after 1 h of pressure loading. The COX-2

mRNA level increased after 1 h of loading and the RANKL/OPG ratio increased significantly after 2 h (but not 1 h) of loading. Further study is needed to elucidate the dose and frequency responses to cyclic hydraulic pressures at varied magnitudes and frequencies. Recent study suggests that the osteocytes may experience up to 5 MPa fluid pressure under 1000 microstrain loading at 1 Hz [27]. Systematic examination of the effects of CHP on osteocytes will lead toward a better understanding and consequently better controlling of bone remodeling for the treatments of bone diseases and the enhancement of bone health.

## Acknowledgments

This research is supported by NSERC, CFI (Lidan You), and National Institute of Health (AR054385) (Liyun Wang). The confocal microscopy facility image capture was generously provided by Dr. Christopher M. Yip, and his student Jocelyn Lo at the University of Toronto.

## References

- [1] Frost HM. Skeletal structural adaptations to mechanical usage (SATMU): 1. Redefining Wolff's law: the bone modeling problem. *Anat Rec* 1990;226:403–13.
- [2] Aguirre JI, Plotkin LI, Berryhill SB, Shelton RS, Steward SA, Vyas K, et al. Increased prevalence of osteocyte apoptosis precedes osteoclastic bone resorption and the loss of bone mineral and strength induced by lack of mechanical forces in a murine model of unloading. *J Bone Miner Res* 2004;19:S137–S137.
- [3] Riddle RC, Donahue HJ. From streaming potentials to shear stress: 25 years of bone cell mechanotransduction. *J Orthop Res* 2009;27:143–9.
- [4] Kim CH, Kim KH, Jacobs CR. Effects of high frequency loading on RANKL and OPG mRNA expression in ST-2 murine stromal cells. *BMC Musculoskel Dis* 2009;10.
- [5] Bonivitch AR, Bonewald LF, Ling J, Jiang JX, Nicoletta DP. Direct Correlation of Osteocyte Deformation with Calcium Influx in Response to Fluid Flow Shear Stress. *J Bone Miner Res* 2008;23:S145–S145.
- [6] Robling AG, Niziolek PJ, Baldrige LA, Condon KW, Allen MR, Alam I, et al. Mechanical stimulation of bone in vivo reduces osteocyte expression of Sost/sclerostin. *J Biol Chem* 2008;283:5866–75.
- [7] Siller-Jackson AJ, Burra S, Gu S, Xia X, Bonewald LF, Sprague E, et al. Adaptation of connexin 43-hemichannel prostaglandin release to mechanical loading. *J Biol Chem* 2008;283:26374–82.
- [8] Ponik SM, Triplett JW, Pavalko FM. Osteoblasts and osteocytes respond differently to oscillatory and unidirectional fluid flow profiles. *J Cell Biochem* 2007;100:794–807.
- [9] Bourret LA, Rodan GA. The role of calcium in the inhibition of cAMP accumulation in epiphyseal cartilage cells exposed to physiological pressure. *J Cell Physiol* 1976;88:353–61.
- [10] Bagi C, Burger EH. Mechanical stimulation by intermittent compression stimulates sulfate incorporation and matrix mineralization in fetal mouse long-bone rudiments under serum-free conditions. *Calcified Tissue Int* 1989;45:342–7.
- [11] Imamura K, Ozawa H, Hiraide T, Takahashi N, Shibasaki Y, Fukuhara T, et al. Continuously applied compressive pressure induces bone resorption by a mechanism involving prostaglandin E2 synthesis. *J Cell Physiol* 1990;144:222–8.
- [12] Burger EH, Klein-Nulend J, Veldhuijzen JP. Mechanical stress and osteogenesis in vitro. *J Bone Min Res* 1992;7.
- [13] Brighton CT, Fisher Jr JRS, Levine SE, Corsetti JR, Reilly T, Landsman AS, et al. The biochemical pathway mediating the proliferative response of bone cells to a mechanical stimulus. *J Bone Joint Surg - Ser A* 1996;78:1337–47.
- [14] Kelly PJ, Bronk JT. Venous pressure and bone formation. *Microvasc Res* 1990;39:364–75.
- [15] Qin YX, Kaplan T, Saldanha A, Rubin C. Fluid pressure gradients, arising from oscillations in intramedullary pressure, is correlated with the formation of bone and inhibition of intracortical porosity. *J Biomech* 2003;36:1427–37.
- [16] Klein-Nulend J. Increased calcification of growth plate cartilage as a result of compressive force in vitro. *Arthritis Rheum* 1986;29:1002.
- [17] Klein-Nulend J. Inhibition of osteoclastic bone resorption by mechanical stimulation in vitro. *Arthritis Rheum* 1990;33:66.
- [18] Tanck E, Van Driel WD, Hagen JW, Burger EH, Blankevoort L, Huiske R. Why does intermittent hydrostatic pressure enhance the mineralization process in fetal cartilage? *J Biomech* 1999;32:153–61.
- [19] Myers KA, Rattner JB, Shrive NG, Hart DA. Hydrostatic pressure sensation in cells: integration into the tensigrity model. *Biochem Cell Biol* 2007;85:543–51.
- [20] Wu MJ. Effects of hydrostatic pressure on cytoskeleton and BMP-2, TGF-beta, SOX-9 production in rat temporomandibular synovial fibroblasts. *Osteoarthritis Cartilage* 2008;16:41.
- [21] Gardinier JD, Majumdar S, Duncan RL, Wang L. Cyclic hydraulic pressure and fluid flow differentially modulate cytoskeleton re-organization in MC3T3 osteoblasts. *Cell Mol Bioeng* 2009;2:133–43.
- [22] Turner CH, Warden SJ, Bellido T, Plotkin LI, Kumar N, Jasiuk I, et al. Mechanobiology of the skeleton. *Sci Signal* 2009;2.
- [23] Burger EH, Klein-Nulend J. Mechanotransduction in bone – role of the lacunocanalicular network. *Faseb J* 1999;13.
- [24] Zhang D, Weinbaum S, Cowin SC. Estimates of the peak pressures in bone pore water. *J Biomech Eng* 1998;120:697.
- [25] Cowin SC, Gailani G, Benalla M. Hierarchical poroelasticity: movement of interstitial fluid between porosity levels in bones. *Philos Trans R Soc A: Math Phys Eng Sci* 2009;367:3401–44.
- [26] Gailani G, Benalla M, Mahamud R, Cowin SC, Cardoso L. Experimental determination of the permeability in the lacunar-canalicular porosity of bone. *J Biomech Eng* 2009;131:101007.
- [27] Gardinier JD, Townend CW, Jen K-P, Duncan RL, Wang L. In situ permeability measurement of the mammalian lacunar-canalicular system. *Bone* 2010;1:371.
- [28] Berridge MJ, Lipp P, Bootman MD. The versatility and universality of calcium signalling. *Clin Orthop Relat R* 1995;256–69.
- [29] Hung CT, Pollack SR, Reilly TM, Brighton CT. Real-time calcium response of cultured bone cells to fluid flow. *Clin Orthop Relat R* 1995;256–69.
- [30] Adachi T, Aonuma Y, Tanaka M, Hojo M, Takano-Yamamoto T, Kamioka H. Calcium response in single osteocytes to locally applied mechanical stimulus: differences in cell process and cell body. *J Biomech* 2009;42:1989–95.
- [31] Myers KA, Rattner JB, Shrive NG, Hart DA. Osteoblast-like cells and fluid flow: cytoskeleton-dependent shear sensitivity. *Biochem Biophys Res Co* 2007;364:214–9.
- [32] Pavalko FM, Chen NX, Turner CH, Burr DB, Atkinson S, Hsieh YF, et al. Fluid shear-induced mechanical signaling in MC3T3-E1 osteoblasts requires cytoskeleton-integrin interactions. *Am J Physiol - Cell Physiol* 1998;275:1591–601.
- [33] Kawata A, Mikuni-Takagaki Y. Mechanotransduction in stretched osteocytes – temporal expression of immediate early and other genes. *Biochem Biophys Res Co* 1998;246:404–8.
- [34] Tian XY, Zhang Q, Zhao R, Setterberg RB, Zeng QQ, Iturria SJ, et al. Continuous PGE2 leads to net bone loss while intermittent PGE2 leads to net bone gain in lumbar vertebral bodies of adult female rats. *Bone* 2008;42:914–20.
- [35] Boyle WJ, Simonet WS, Lacey DL. Osteoclast differentiation and activation. *Nature* 2003;423:337–42.
- [36] Burger EH, Klein-Nulend J, Smit TH. Strain-derived canalicular fluid flow regulates osteoclast activity in a remodelling osteon – a proposal. *J Biomech* 2003;36:1453–9.
- [37] Aguirre JI, Plotkin LI, Stewart SA, Weinstein RS, Parfitt AM, Manolagas SC, et al. Osteocyte apoptosis is induced by weightlessness in mice and precedes osteoclast recruitment and bone loss. *J Bone Miner Res* 2006;21:605–15.
- [38] Aguirre J, Plotkin L, Vyas K, Stewart S, O'Brien C, Parfitt A, et al. Osteocyte apoptosis and the loss of bone mineral and strength induced by tail suspension in mice is entirely caused by reduced mechanical strains, whereas osteoblast apoptosis is due to endogenous glucocorticoid actions. *J Bone Miner Res* 2005;20:S24–S24.
- [39] Hung CT, Allen FD, Pollack SR, Brighton CT. Intracellular Ca2+ stores and extracellular Ca2+ are required in the real-time Ca2+ response of bone cells experiencing fluid flow. *J Biomech* 1996;29:1411–7.
- [40] Klein-Nulend J. Mechanical stimulation of osteopontin mRNA expression and synthesis in bone cell cultures. *J Cell Physiol* 1997;170:174.
- [41] Nagatomi J, Arulanandam BP, Metzger DW, Meunier A, Bizios R. Frequency- and duration-dependent effects of cyclic pressure on select bone cell functions. *Tissue Eng* 2001;7:717–28.
- [42] Roelofsen J. Mechanical stimulation by intermittent hydrostatic compression promotes bone-specific gene expression in vitro. *J Biomech* 1995;28:1493.
- [43] Takai E, Mauck RL, Hung CT, Guo XE. Osteocyte viability and regulation of osteoblast function in a 3D trabecular bone explant under dynamic hydrostatic pressure. *J Bone Miner Res* 2004;19:1403.
- [44] Klein-Nulend J, Van der Plas A, Semeins CM, Ajubi NE, Frangos JA, Nijweide PJ, et al. Sensitivity of osteocytes to biomechanical stress in vitro. *FASEB J* 1995;9:441–5.
- [45] Jacobs CR, Yellowley CE, Davis BR, Zhou Z, Cimbala JM, Donahue HJ. Differential effect of steady versus oscillating flow on bone cells. *J Biomech* 1998;31:969–76.
- [46] Awrangjeb M, Lu G. Robust image corner detection based on the chord-to-point distance accumulation technique. *IEEE T Multimedia* 2008;10:1059–72.
- [47] Zhou Q, Zhao J, Stout JG, Luhm RA, Wiedmer T, Sims PJ. Molecular cloning of human plasma membrane phospholipid scramblase. *J Biol Chem* 1997;272:18240–4.
- [48] Murakami M, Naraba H, Tanioka T, Semmyo N, Nakatani Y, Kojima F, et al. Regulation of prostaglandin E2 biosynthesis by inducible membrane-associated prostaglandin E2 synthase that acts in concert with cyclooxygenase-2. *J Biol Chem* 2000;275:32783–92.
- [49] Langenbach R, Morham SG, Tian HF, Loftin CD, Ghanayem BI, Chulada PC, et al. Prostaglandin synthase 1 gene disruption in mice reduces arachidonic acid-induced inflammation and indomethacin-induced gastric ulceration. *Cell* 1995;83:483–92.
- [50] Dinchuk JE, Car BD, Focht RJ, Johnston JJ, Jaffee BD, Covington MB, et al. Renal abnormalities and an altered inflammatory response in mice lacking cyclooxygenase II. *Nature* 1995;378:406–9.
- [51] Kamioka H, Sugawara Y, Murshid SA, Ishihara Y, Honjo T, Takano-Yamamoto T. Fluid shear stress induces less calcium response in a single primary osteocyte than in a single osteoblast: implication of different focal adhesion formation. *J Bone Miner Res* 2006;21:1012–21.
- [52] Gomis A, Soriano S, Belmonte C, Viana F. Hypoosmotic- and pressure-induced membrane stretch activate TRPC5 channels. *J Physiol* 2008;586:5633–49.
- [53] You J, Reilly GC, Zhen X, Yellowley CE, Chen Q, Donahue HJ, et al. Osteopontin gene regulation by oscillatory fluid flow via intracellular calcium mobilization and activation of mitogen-activated protein kinase in MC3T3-E1 osteoblasts. *J Biol Chem* 2001;276:13365–71.
- [54] Chen NX, Geist DJ, Genetos DC, Pavalko FM, Duncan RL. Fluid shear-induced NF- $\kappa$ B translocation in osteoblasts is mediated by intracellular calcium release. *Bone* 2003;33:399–410.
- [55] Buljan V, Ivanova EP, Cullen KM. How calcium controls microtubule anisotropic phase formation in the presence of microtubule-associated proteins in vitro. *Biochem Biophys Res Co* 2009;381:224–8.

- [56] Brangwynne CP, MacKintosh FC, Kumar S, Geisse NA, Talbot J, Mahadevan L, et al. Microtubules can bear enhanced compressive loads in living cells because of lateral reinforcement. *J Cell Biol* 2006;173:733–41.
- [57] Gross M, Jaenicke R. Proteins under pressure. The influence of high hydrostatic pressure on structure, function and assembly of proteins and protein complexes. *Eur J Biochem* 1994;221:617–30.
- [58] O'Brien ET, Salmon ED, Erickson HP. How calcium causes microtubule depolymerization. *Cell Motil Cytoskelet* 1997;36:125–35.
- [59] McGarry JG, Klein-Nulend J, Prendergast PJ. The effect of cytoskeletal disruption on pulsatile fluid flow-induced nitric oxide and prostaglandin E2 release in osteocytes and osteoblasts. *Biochem Biophys Res Commun* 2005;330:341–8.
- [60] Staves MP, Wayne R, Leopold AC. Hydrostatic pressure mimics gravitational pressure in characean cells. *Protoplasma* 1992;168:141–52.
- [61] Bonewald LF, Johnson ML. Osteocytes, mechanosensing and Wnt signaling. *Bone* 2008;42:606–15.
- [62] Gao Q, Zhan P, Alander CB, Kream BE, Hao C, Breyer MD, et al. Effects of global or targeted deletion of the EP4 receptor on the response of osteoblasts to prostaglandin in vitro and on bone histomorphometry in aged mice. *Bone* 2009;45:98–103.
- [63] Jee WSS, Ke HZ, Li XJ. Long-term anabolic effects of prostaglandin-E2 on tibial diaphyseal bone in male rats. *Bone Miner* 1991;15:33–55.
- [64] Minamizaki T, Yoshiko Y, Kozai K, Aubin JE, Maeda N. EP2 and EP4 receptors differentially mediate MAPK pathways underlying anabolic actions of prostaglandin E2 on bone formation in rat calvaria cell cultures. *Bone* 2009;44:1177–85.
- [65] Jee WSS, Ma YF. The in vivo anabolic actions of prostaglandins in bone. *Bone* 1997;21:297–304.
- [66] Gao Q, Xu M, Alander CB, Choudhary S, Pilbeam CC, Raisz LG. Effects of prostaglandin E2 on bone in mice in vivo. *Prostaglandin Oth Lipid Med* 2009;89:20–5.
- [67] Hughes-Fulford M. Signal transduction and mechanical stress. Science's STKE [electronic resource]: signal transduction knowledge environment 2004; 2004.
- [68] Zhao S, Kato Y, Zhang Y, Harris S, Ahuja SS, Bonewald LF. MLO-Y4 osteocyte-like cells support osteoclast formation and activation. *J Bone Miner Res* 2002;17:2068–79.
- [69] Silvestrini G, Ballanti P, Patacchioli F, Leopizzi M, Gualtieri N, Monnazzi P, et al. Detection of osteoprotegerin (OPG) and its ligand (RANKL) mRNA and protein in femur and tibia of the rat. *J Mol Histol* 2005;36:59–67.
- [70] Glass LI, Bialek P, Ahn JD, Starbuck M, Patel MS, Clevers H, et al. Canonical Wnt signaling in differentiated osteoblasts controls osteoclast differentiation. *Dev Cell* 2005;8:751–64.
- [71] You L, Temiyasathit S, Lee P, Kim CH, Tummala P, Yao W, et al. Osteocytes as mechanosensors in the inhibition of bone resorption due to mechanical loading. *Bone* 2008;42:172–9.
- [72] Tan SD, Kuijpers-Jagtman AM, Semeins CM, Bronckers ALJJ, Maltha JC, Von den Hoff JW, Everts V, Klein-Nulend J. Fluid shear stress inhibits TNF alpha-induced osteocyte apoptosis. *J Dent Res* 2006;85:905–9.
- [73] Plotkin LI, Mathov I, Aguirre JI, Parfitt AM, Manolagas SC, Bellido T. Mechanical stimulation prevents osteocyte apoptosis: requirement of integrins, Src kinases, and ERKs. *Am J Physiol-Cell Physiol* 2005;289:C633–43.
- [74] Kitase Y, Johnson ML, Bonewald LF. The protective effects of mechanical strain on osteocyte viability is mediated by the effects of prostaglandin on the cAMP/PKA and the beta-catenin pathways. *J Bone Miner Res* 2007;22:S178–9.